

Chapter 25 [In: *Natural Gas Hydrate, in Oceanic and Permafrost Environments*. M.D. Max, Ed. Kluwer Publ., 2000.]**Laboratory synthesis of pure methane hydrate suitable for measurement of physical properties and decomposition behavior.**

Laura A. Stern¹, Stephen H. Kirby¹, William B. Durham², Susan Circone¹, and William F. Waite¹

¹U.S. Geological Survey, MS/ 977, Menlo Park, CA 94025

²U.C. Lawrence Livermore National Laboratory, Livermore, CA 94550

1. INTRODUCTION AND BACKGROUND**1.1 Why study synthetic gas hydrates?**

Gas hydrates are an intriguing class of nonstoichiometric compounds that have significant commercial and scientific applications both as an energy resource and as a manufactured material. The last half-century has witnessed a marked escalation in the scope of experimental research on gas hydrates, particularly directed towards the determination of their phase equilibria, formation kinetics, crystallographic and structural properties, transport and thermal properties, effects of inhibitors, and a number of related geochemical topics.

There remains, however, a paucity of reliable experimental measurements of many of the physical, material, thermal, acoustic, and elastic properties of most pure, end-member hydrocarbon hydrates. Instead, either water ice, or hydrates readily formed in the laboratory but rarely occurring in nature (such as ethylene-oxide hydrate and THF hydrate), have commonly been used as analogue material for property measurements. Consequently, there does not exist an accurate and comprehensive database of physical and material properties for end-member gas hydrates, and particularly for those hydrates that are more problematic to form and stabilize in the laboratory. Compounding this problem is the difficulty in retrieving pristine material from natural settings on which to make such measurements, in different laboratories using different methods, and in the general lack of agreement of measurements made on synthetic material.

A wide variety of processes and techniques have been used to synthesize gas hydrates in the laboratory, each yielding a final product that may be highly suitable for some types of experimental testing while clearly unsuitable for others. Here, we focus on laboratory production of pure, polycrystalline methane hydrate and hydrate-sediment aggregates that are suitable for a variety of physical and material properties measurements made on pure, end-member material. The methods described here are based on a materials-science approach

that strives to produce final test specimens with highly-reproducible composition, texture, and grain characteristics. Property measurements on such test specimens not only provide end-member material characterization, but also aid in the interpretation of similar measurements made on more complicated hydrate-bearing material retrieved from natural settings.

1.2 Criteria for sample suitability.

Historically, bulk quantities of gas hydrates have been produced in many laboratories by a variety of different methods, commonly mimicking either hydrate-forming processes that are thought to occur in nature, or under conditions of pressure and temperature that may occur in nature. Many researchers have grown gas hydrate by bubbling a hydrate-forming gas through seawater- or freshwater-saturated sediment columns, simulating ocean-floor type conditions or processes. Others have produced hydrates from ice + gas mixtures by vigorous agitation, shaking, or rocking procedures that continually renew fresh ice surfaces for hydrate growth. An excellent and comprehensive review of a variety of methods and fabrication apparatus is given by Sloan (1998, chapter 6), to which we refer the reader for further background information.

While the material produced by such dynamic methods may be suitable for some types of measurements, particularly those related to phase equilibria, formation processes, and formation kinetics, there remain some outstanding problems inherent to these procedures which render the resulting material less suitable for those measurements in which precise knowledge and excellent reproducibility of composition and grain characteristics are required. These problems include: (1) The resulting hydrate customarily includes excess or unreacted H₂O, either as liquid water or as ice, which is difficult to separate and remove from the final hydrate product. Not only does excess H₂O contaminate the hydrate and influence all subsequent property measurements, but it also greatly hinders accurate determination of the composition and stoichiometry of the resulting hydrate. (2) Hydrate produced by continuous agitation methods has generally been produced under low to moderate pressures, resulting in low methane content in the resulting hydrate. (3) Synthetic hydrate formed from water or from continually-agitated ice grains does not have well constrained or well controlled grain size, grain texture, or crystallographic orientation, parameters which can strongly affect those properties influenced by grain anisotropy, such as ductile flow behavior or elastic properties.

We present here an alternative method for efficient and routine synthesis of pure methane hydrate in a form that is highly suitable as a standard for properties measurement. We review an *in situ* "seeding" method for hydrate nucleation and growth, a procedure developed from extensive work on other H₂O-based icy compounds in which we demonstrated successful growth of polycrystalline test specimens with controlled and uniform grain size, and with no preferred crystallographic orientation or anisotropy effects (Durham et al., 1983, 1993). Similarly, gas hydrate samples produced by this method are highly reproducible from sample-to-sample in terms of known purity, composition,

stoichiometry, porosity, grain size, and grain orientation. Such sample characteristics are not only necessary for reliable characterization of the intrinsic properties of crystalline solids, but individual parameters can then be changed in a controlled manner for systematic modeling of increasingly complex systems.

This latter point makes the seeding method particularly effective for laboratory modeling of natural systems, as sediment and impurity effects are difficult to isolate in measurements made on natural hydrate-bearing samples due to the inherent complexity of the material and the slow recovery process. Ocean-sediment hydrates recovered from drill core may contain, for example, partially-decomposed hydrate with poorly known stoichiometry, composition, and grain size; excess water or ice produced from partial dissociation; additional pore water; poorly constrained sediment compositions, distributions, grain size and grain orientations; poorly known grain boundary contacts or "cementing" contacts; and possible additional components such as carbonate mineralization or organic detritus. Our seeding procedure allows for easy pre-mixing or layering of a wide variety of particulate matter to the granulated ice prior to converting the ice to gas hydrate, thus enabling fabrication of "tailored" hydrate/sediment aggregates of varying complexity.

1.3 Focus of this chapter: Three basic aspects of gas hydrate synthesis and properties measurements are covered in this chapter. (1) Synthesis apparatus and techniques used for growth of pure, polycrystalline methane hydrate samples, hydrate + sediment ± seawater composites, and hydrates made from liquid hydrocarbons or multi-component systems. Observations of methane hydrate formation from ice grains and a possible model for the reaction are also discussed, as well as key factors for successful synthesis of gas hydrates and for scaling up of sample size. (2) Apparatus and techniques used for measuring stoichiometry, composition, annealing effects, stability, and dissociation rates and kinetics. (3) Applications for property measurements, and apparatus modifications to accommodate compaction and *in situ* measurement of physical, thermal, mechanical, and acoustic properties.

2. SYNTHESIS PROCEDURES AND APPARATUS

2.1 Pure methane hydrate.

Samples of polycrystalline methane hydrate can be efficiently synthesized by promoting the general reaction $\text{CH}_4 (\text{gas}) + 6\text{H}_2\text{O} (\text{sol.} \rightarrow \text{liq.}) \rightarrow \text{CH}_4 \cdot 6\text{H}_2\text{O} (\text{sol.})$ (Fig. 1). This product is achieved by the mixing and subsequent slow, regulated heating of sieved, granular, H_2O "seed" ice and cold, pressurized CH_4 gas in an approximately constant-volume reaction vessel (Fig. 2). This seeding method for hydrate nucleation and growth permits successful synthesis of polycrystalline test specimens with controlled and uniform grain size with no detectable preferred crystallographic orientation, which we have verified through sample-replica observation and powder x-ray analysis (Stern et al., 1998a).

Sample fabrication details are as follows: CH_4 gas from a source bottle is initially boosted in pressure (P) by a gas intensifier and routed into sample

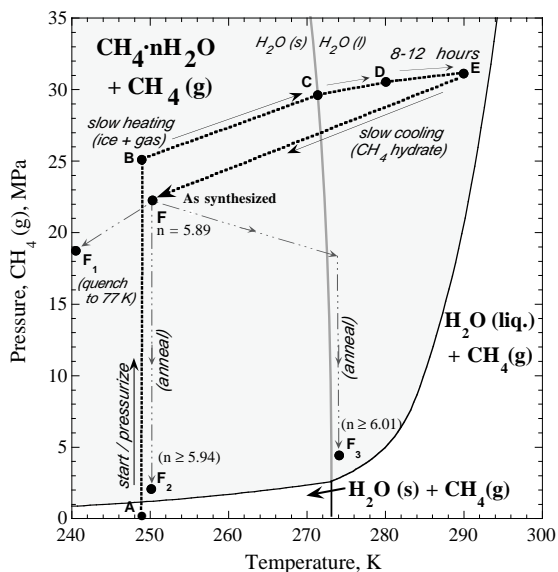


Figure 1: Methane hydrate synthesis and annealing conditions in relation to the CH_4 - H_2O phase diagram. Shaded region shows methane hydrate stability field. The metastable extension of the H_2O melting curve is shown by the solid grey curve. Black dotted lines trace the reaction path during methane hydrate synthesis from ice + gas mixtures. Points A-F indicate the P-T path during reaction. For synthesis, H_2O "seed" ice at 250 K (pt. A) is pressurized with CH_4 gas to 25 MPa (B). Heating the mixture through the H_2O melting point (C) and up to 290 K (C-D-E) promotes full and efficient conversion of the ice to gas hydrate. Samples are then cooled to 250 K (F), and can then be quenched (F_1) and removed from the apparatus, or annealed at conditions closer to the equilibrium curve (F_2 , F_3). The "n" numbers represent hydrate stoichiometry under various conditions.

molding vessels housed in a conventional deep freezer. The sample assembly (Fig. 2) consists of a manifold of as many as four stainless steel vessels immersed in an ethyl alcohol bath initially held at freezer temperature of ~ 250 K. One vessel serves as a reservoir to store and chill pressurized CH_4 gas, and the others contain the sample molds. Each mold consists of a hollow split-cylinder that encases an indium sleeve filled with a measured mass of H_2O "seed" ice typically packed to 40% porosity. Seed material is made from a gas-free and nearly single-crystal block of ice grown from triply distilled H_2O , crushed, ground, and sieved to 180-250 μm grain size (Durham et al., 1983). The sample vessels with seed ice are initially closed off from the reservoir and evacuated. A disk inserted on top of the packed ice grains prevents displacement of the ice during evacuation. Multiple thermocouples inserted into the base of either sample prior to loading of the ice permit careful monitoring of the sample's thermal history during synthesis and subsequent testing. A Heise pressure gauge and pressure transducers monitor gas pressure on the samples.

The reservoir vessel is first charged with pressurized CH_4 gas to 35 MPa and cooled to 250 K. When fabricating a single sample, the reservoir is opened to the pre-evacuated sample chamber and methane pressure (P_{CH_4}) drops to ~ 24 MPa. For fabrication of multiple samples, the reservoir charging, cooling, and opening procedures are repeated to bring the larger volume of the multiple-sample system to about 25 MPa at 250 K. These steps serve to fill the porosity between the ice grains to a molar ratio of CH_4 to H_2O well in excess of that required for complete hydrate reaction. The bath temperature can then be slowly raised by various methods such as by use of a ring immersion heater or a simple hot plate located beneath the alcohol bath. As the samples and gas reservoir warm, they self-pressurize by thermal expansion. Up to 271 K, methane gas pressure (P_{CH_4}) increases approximately linearly with increasing temperature, following a slope governed primarily by the equilibrium thermal expansion of

free CH_4 in the system. Measurable reaction begins as temperature rises above 271.5 K (the approximate melting point of ice at our synthesis pressure), and consumption of CH_4 gas by hydrate formation slows the rate of P_{CH_4} increase (Fig. 3). Progress of the hydrate-forming reaction is monitored by observing the deflection of P from the initially linear P - T curve. Completion of reaction is efficiently achieved by steady heating to $\sim 289 \pm 1$ K over a heating time interval of about 12 to 15 hours after the sample vessel crosses the 271.5 K isotherm (Fig. 3). Data-acquisition software (LabVIEWTM, National Instruments) monitors and records the P - T conditions throughout each run. The extent of reaction can be determined mid-run by the measured P_{CH_4} offset from the reversible CH_4 expansion curve.

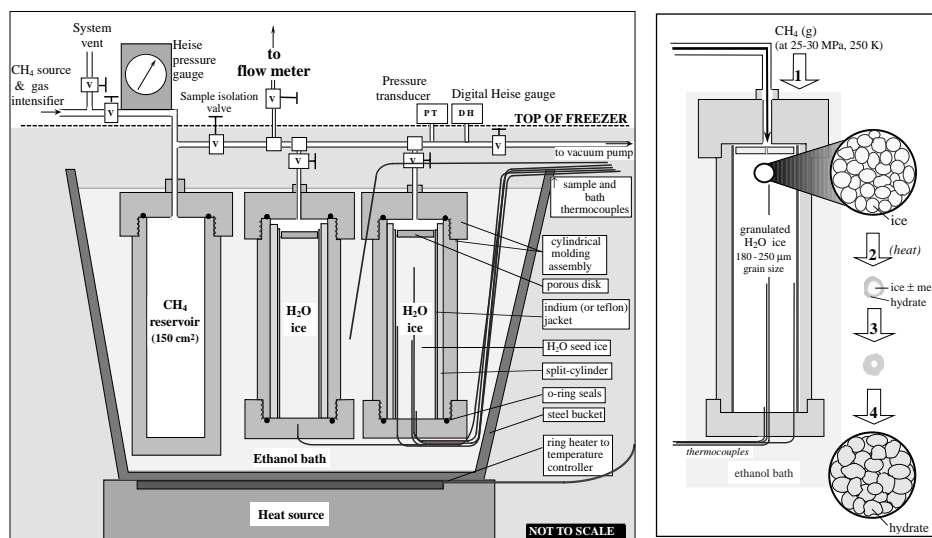


Figure 2: Left: Apparatus for synthesizing test specimens of pure, polycrystalline methane hydrate from CH_4 gas and H_2O ice by methods described in text. Right: Postulated synthesis model. Numbered arrows (1-4) are as follows: 1) Cold, pressurized methane gas (35 MPa, 250 K) is admitted to the ice in the sample chamber. The reactants equilibrate to ~ 25 MPa and 250 K. 2) Warming above the H_2O melting point initiates measurable hydrate formation along the surface of the ice grains, creating composite grains in which a mantle of hydrate envelops an unreacted ice (\pm melt) core. The reaction rate (diffusion or transport controlled) slows as the hydrate rind grows and thickens, and the inner unreacted core shrinks. 3) Slowly raising the temperature to 290 K promotes further reaction. 4) By the end of the heating cycle, the reaction has reached completion.

Following full reaction, the heat source is turned off, and the system slowly cools through the freezing point of ice and down to freezer temperature (~ 250 K). At this stage, the P - T record should be inspected for any indication of a freezing anomaly during the cooling cycle, signifying incomplete reaction. Such an anomaly appears as a discontinuous jump in both the P and T readings at several degrees below 273 K, produced when small amounts of unreacted and supercooled water suddenly freeze to form ice (see Fig. 6 in Stern et al., 1998a,

for example). The exothermic process of freezing even very small amounts of water (< 1.5 vol. %), coupled with the associated volume increase, is easily measured by the internal thermocouples and pressure transducers. The presence of such discontinuities requires cycling the sample through the melting point of ice a second time to insure completion of reaction.

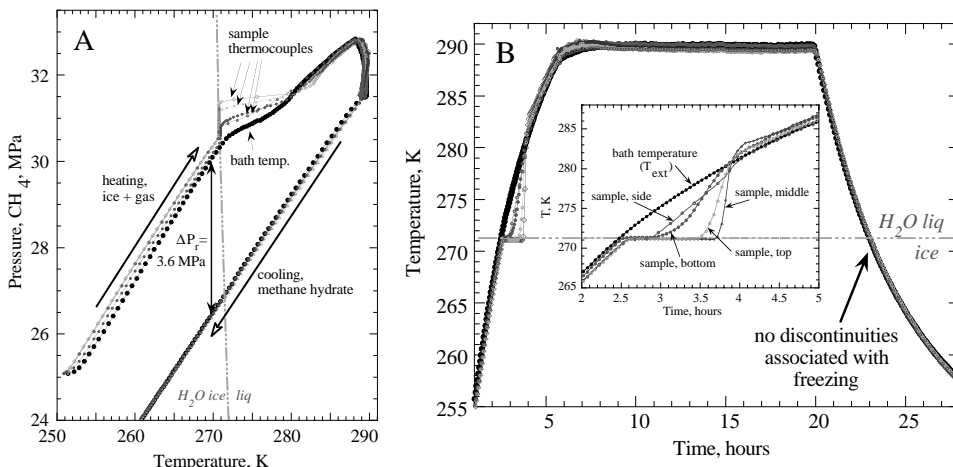


Figure 3. (A) P-T history of a methane hydrate synthesis run (with two samples) during the reaction: $\text{CH}_4(\text{g}) + 5.9\text{H}_2\text{O}(\text{ice} \rightarrow \text{melt}) \rightarrow \text{CH}_4 \cdot 5.9\text{H}_2\text{O}$. Warming the ice + gas mixture above the H_2O solidus (dot-dashed line) initiates measurable reaction. Increasing temperature slowly to 290 K, over an 8-15 hour span, promotes full reaction. Complete reaction is marked by a known pressure drop (ΔP_r) from start to finish relative to the extrapolated subsolidus P-T curve. (B) Temperature-time profile during hydrate formation. The thermal profile of the sample as it warms through the H_2O melting point is expanded in the inset. Buffering of the sample thermocouples at the H_2O melting point indicates that a measurable fraction of melting of the seed ice occurs over this 1.2 hour stage. Full conversion of the H_2O to hydrate requires 8-12 hours however, and ΔP_r over the early melting stage is not as large as that predicted for complete melting of all residual ice (see Fig. 3A in Stern et al., 1996, for further details).

If no refreezing anomaly appears, samples may then be annealed, tested, or removed from the apparatus. For removal, samples should be vented to low P_{CH_4} within the hydrate field (~ 2 MPa at 250 K), then slowly depressurized while cooled with liquid nitrogen. Pressure must be maintained on the sample to keep the gas hydrate within its stability field during the initial phase of the cooling procedure down to 190 K, but the sample should be fully vented before it cools through 109 K, where any residual pressurized methane in the pore space will liquefy. Allowing liquid methane to settle and freeze as the sample is further cooled to liquid nitrogen temperature (77 K) results in a final material that is mildly explosive and very difficult to work with when rewarmed. Following the quenching procedure, the vessels can be disconnected from the apparatus and opened. The inner, hollow split-cylinders containing the jacketed samples are pushed out of the vessels and pried off the samples. Samples are then wrapped tightly in Al foil and stored in or directly above liquid nitrogen.



Figure 4. Cylindrical test specimens of polycrystalline methane hydrate and mixed sediment aggregates grown by methods described in the text. **Left:** Sample of pure methane hydrate ($\text{CH}_4 \cdot 5.89\text{H}_2\text{O}$), 2.54 cm x 11.5 cm, with uniform grain size of ~ 300 microns and approximately 28% porosity. The encapsulating indium jacket in which the sample was grown has been split and peeled back from the sample. **Right:** Pure methane hydrate + sediment aggregates fabricated with pre-specified characteristics. Samples are 2.54 cm by 10 - 11.5 cm. Sample at left is methane hydrate + pure quartz sand, varying the proportion of sand in each quarter of the sample. Middle and right samples are mixtures of pure methane hydrate and 1.25 ± 0.25 mm black Al_2O_3 particulate. The two samples containing Al_2O_3 were grown in Teflon jackets (split along top surface) rather than in indium jackets.

The resulting material is a cohesive aggregate of uniformly fine, equant, white grains of pure methane hydrate with grain clusters of $250 \pm 50 \mu\text{m}$ grain size (Fig. 4). Samples that were initially packed to 40% porosity will contain $29 \pm 1\%$ porosity after full reaction due to the volume increase accompanying conversion of the ice to gas hydrate. Purity of the final material and efficiency of the synthesis are highly dependent on adhering to certain key procedures, discussed below. Careful measurements of gas released from fully reacted samples show that the gas hydrate produced at the prescribed test conditions has a highly-reproducible composition of $\text{CH}_4 \cdot n\text{H}_2\text{O}$, where $n = 5.89 \pm 0.01$.

2.2 Methane hydrate + sediment (\pm seawater) aggregates.

Test specimens of methane hydrate + sediment mixtures are easily produced by pre-mixing or layering sediments with granular ice in each reaction

vessel prior to admission of CH₄ gas. With the static growth method, there is no migration of either H₂O or sediment in pre-mixed samples, so samples can be "customized" to any desired mixture or layering sequence. To date, samples have been successfully made with pure methane hydrate inter-layered with discrete horizons of particulate material with grain size as fine as 50 μm (using SiC) and as coarse as 2 mm (using Al₂O₃), with no discernable change in the layering during synthesis (Fig. 4). Alternatively, sediments can be homogeneously mixed with seed ice before synthesis to produce a final product that remains fully mixed.

Saturating the gas hydrate or hydrate/sediment samples with seawater (or fresh water) immediately following synthesis is possible but somewhat problematic, in that it can be difficult to assess the extent and distribution of any secondary gas hydrate growth resulting from the added water. A simple method for saturation involves first depressurizing the sample to P-T conditions that are slightly warmer than the ice point but close to equilibrium conditions (for instance, 275 K and 3 MPa P_{CH₄}), then admitting highly pressurized seawater through the upper port of the sample such that the pressurized head space over the water pushes the water into the sample and then gravitationally floods the available pore space. Use of the same hydrate-forming gas to pressurize the water prevents possible contamination of the sample due to entrainment or dissolution of the pressurizing gas within the water. Monitoring the weight changes of both the sample and H₂O reservoir enables determination of the mass of H₂O incorporated into the sample. A more optimal procedure involves a flow-through design to facilitate full saturation of all available pore volume with the added water, easily determined by flowing the water through the base of the sample and observing its emergence from the top end of the sample.

2.3 Methane hydrate formation from melting ice; direct observations, and factors for complete reaction.

Hydrate formation and growth processes can be further investigated by optical microscopy, using a simple and versatile optical cell constructed from standard high-pressure valve bodies and SiO₂ capillary tubing (Fig. 1 in Chou et al., 1990). This design was used for observing methane hydrate growth from seed ice, by chilling the cell and loosely filling it with 200 μm ice grains prepared identically to those used in standard samples. The pore volume was then evacuated and flooded with cold CH₄ gas at 23 MPa and 250 K. The cell was then immersed in an insulated dish of cold ethanol, placed under the microscope, and slowly warmed from 250 K to 290 K.

Ice grains subjected to CH₄ hydrate-forming conditions showed visible surface reaction at temperatures well below the H₂O liquidus, almost immediately after exposure to CH₄ gas. This surface appearance did not change appreciably as the grains were subsequently warmed through the H₂O liquidus. Upon further heating, no expulsion of water was observed nor any cracking or collapsing of the hydrate encasement that would be expected to attend the volume contraction associated with bulk melting of the ice interiors. Instead, all

grains maintained identifiable shapes and sizes throughout reaction, and changed only by becoming increasingly mottled in appearance as they approached full conversion to hydrate. In separate experiments in which the hydrate was slowly heated and then cycled through the equilibrium curve, however, newly-formed gas hydrate always grew as optically clear material, either coarsely crystalline or as single crystals. Further details and photographs of these experiments are given in Stern et al., (1998b).

At low temperatures in the ice subsolidus field, hydrate formation on ice grains virtually halts (on the laboratory time scale) after initial surface reaction unless the grains are vigorously agitated to renew fresh surfaces for gas hydrate formation. The process of converting the unreacted core to hydrate by raising the temperature, however, is less well understood. We previously hypothesized that the rapid hydrate formation promoted by raising the temperature well above the melting point of ice, in the absence of measurable bulk melting and melt segregation, continues by an essentially solid-state transport or diffusion-controlled reaction (Fig. 2; also Stern et al., 1996, 1998a, 1998b). We speculated that our synthesis conditions promote transport of methane through the outer hydrate rind and inward to the hydrate/ice interface at a rate sufficiently fast such that melt nuclei react to form hydrate faster than they can grow to the critical size necessary for bulk melting and melt segregation. If the rate of bulk melting of the ice can be suppressed by continual removal of melt nuclei, this suggests, by corollary, the possible short-term "superheating" of the ice.

In previous work we noted that while all samples synthesized at 27-32 MPa do in fact show evidence for some melting of the ice cores as the system is initially warmed through the melting point of ice, no evidence was observed to indicate complete melting or melt segregation, even though full conversion of ice to gas hydrate requires about 8 hours by our methods (Stern et al., 1996, 1998a). This early melting stage is now detected with improved accuracy with the multiple-thermocouple design of the reaction vessels that allow significantly improved detection of the thermal lag produced by the latent heat of melting (Fig. 3B). These measurements show that the melt stage is more significant than previously calculated, but still do not indicate either complete or rapid melting of all the unreacted ice in the system immediately upon crossing the ice point.

Further testing is clearly required to better resolve the questions surrounding hydrate formation from slowly-melting ice grains, and whether or not unreacted ice can exist temporarily in a superheated state. Recent NMR imaging reported by Moudrakovski et al., (1999) on hydrate formation from melting ice grains at lower methane pressures (< 12 MPa) showed that in fact particle morphology can be maintained when rinds of hydrate encapsulate an inner core of melt. Similar studies have not yet been conducted at the high P and T conditions of our synthesis procedures, however.

2.3.1 Key factors for successful synthesis of pure methane hydrate. The synthesis procedures described here appear to be highly dependent on those aspects that influence the availability, transport, and concentration of gas-

hydrate-forming species at the growth front. These factors include elevated P-T conditions, and a high surface-to-volume ratio of the reacting grains to minimize the thickness of the developing hydrate layer through which the reactants must pass.

In terms of the procedures described here, the following three experimental parameters are integral to the full and efficient conversion of ice to gas hydrate without measurable segregation of a bulk melt phase: (1) maintenance of a very high methane overpressure above the methane hydrate equilibrium curve (25-33 MPa), (2) moderate thermal ramping (~ 5 -12 K/hr) and subsequent holding of temperature at very warm conditions (288-290 K for 8-12 hours), and (3) using a small initial grain size of seed material ($< 300 \mu\text{m}$). Synthesis tests conducted with larger grain sizes of seed ice (0.5-2 mm) or lower overpressures of CH_4 (4-11 MPa) resulted in only partial reaction, measurable bulk melting, and significant segregation and pooling of the melt into the lower region of the sample chamber (Stern et al., 1998a, 1998b). Thermal ramping to lower temperatures ($< 285 \text{ K}$) or with very slow ramping rates ($< 3 \text{ K/hr}$) also reduced the efficiency of the reaction process, and commonly resulted in incomplete reaction and melt segregation. For samples in which melt segregation occurs, it is troublesome and very inefficient to convert the segregated melt phase to gas hydrate under static conditions. Multiple cyclings through the ice point are required, but may still result in a substandard final material. Finally, we note that successful conversion of ice grains to hydrate grains may also be specific to our method for preparing the ice in order to minimize defects, impurities, or grain boundaries that can act as sites for melt nuclei, but this aspect of sample preparation is as yet unverified.

2.3.2 Considerations for scaling up to larger sample sizes.

The methods and apparatus discussed in this chapter can be adapted to synthesize material in a variety of sample configurations or scaled up significantly in size. Those factors that affect the rate of reaction and/or the heat flow budget of the system, however, should be given careful consideration to best assess appropriate apparatus modifications to ensure successful fabrication of the desired end-product. Using a gas reservoir chamber that has not been scaled up with an increased sample size, for instance, will affect the relative pressure drop due to the reaction, that in turn can result in partial melting of the sample or affect its thermal state.

Other factors that we have identified in preliminary tests include extremely rapid thermal ramping ($>20 \text{ K/hr}$) up to peak temperatures, and synthesizing large samples with low surface-to-volume ratios, both of which can result in heat transfer problems during synthesis due to insufficient dissipation of the exothermic heat of the gas-hydrate-forming reaction. In several cases, the internal sample temperature was observed to significantly overshoot the external bath temperature due to an insufficient rate of heat transfer, resulting from the low thermal conductivity of the newly-forming hydrate and the porous nature of the sample.

Simple methods to circumvent these problems include (1) using a sufficiently large fluid bath surrounding the sample chambers to permit adequate heat transfer and thermal stabilization. (2) Increasing the surface-to-volume ratio of oversized samples to alleviate heat transfer problems. (3) Controlling or moderating the rate of reaction by use of a sufficiently large gas reservoir during synthesis to maintain high gas overpressures during synthesis (the reservoir-to-sample chamber volume ratio should not be less than about 2:1), and by using a moderate thermal ramping rate (5-15 K/hr). (4) Incorporating sediments and/or seawater into large samples to aid in heat transfer and to decrease the total amount of gas hydrate formed in such samples.

Temperature overshoot in the sample interior may not necessarily be undesirable or detrimental, however, as it can be exploited to drive the system to self-buffer along the equilibrium curve at high P-T conditions, and can result in the development of larger and more optically-translucent grains. It is yet to be determined, however, if such material retains a uniform grain size and lack of crystallographic orientation throughout all regions of the sample.

2.4 Synthesis from liquid hydrocarbons or multi-component systems.

Synthesis of pure gas hydrates from gas phases that liquefy at our synthesis pressures (CO₂, propane, ethane, etc), or from mixed-gas sources in which components can unmix at synthesis conditions, can be achieved with several modifications to the standard procedures. Certain problems require special consideration, however. These include: (1) the difficulty in achieving high P conditions without unmixing a multi-component source gas, and the inability to access and utilize high T conditions due to the steep equilibrium curves of the phase diagrams for many of these types of gas hydrates. (2) Maintaining a homogeneous distribution of phases in the pore space between the ice grains. This maintenance of phases can be a problem when synthesizing mixed-phase gas hydrates, due to the density differences between the various components and/or phases. Similarly, variations in sample stoichiometry can arise even when working with a single component liquid hydrocarbon, if only the lower portion of the sample remains saturated with the liquid phase while the upper portion is saturated with the gas phase. (3) Quenching the final hydrate product to temperatures below the dissociation temperature of the hydrate, without freezing in hydrocarbon phase in the pore space.

To circumvent these difficulties, it is critical to first establish the P-T conditions at which the source gas liquefies, and at what conditions the gas mixture can be delivered from the source bottle while maintaining its original composition. Many pressurized gas mixtures are guaranteed to be deliverable at room T with known composition, but will partially condense, unmix, and pool in the reservoir at freezer T. In such cases it is necessary to cool and deliver the source gas to the samples by a different means than our standard technique.

One method is to move the gas reservoir down-line from the samples, and to place in its original position a tightly-wound cooling coil that is suspended in the alcohol bath and that connects the source bottle to the samples

and reservoir. This configuration allows the source gas to be pre-cooled as it is delivered to the samples, but without letting any liquid settle up-stream of the samples. The samples and reservoir should then all be pressurized in one step.

Alternatively, for single-component systems, a reservoir of pressurized liquid hydrocarbon can be positioned directly above a sample chamber, and the pore space of the ice can then be saturated by using the pressure differential behind the liquid as well as gravitational feed.

Another option for synthesizing mixed-phase gas hydrates that include methane, is to first fully saturate the pore space of the seed ice with the liquid hydrocarbon phase by one of the methods discussed above, and then further pressurizing with methane gas to high pressure (>25 MPa). This method permits accessing higher P-T conditions for synthesis, due to the shift in dissociation conditions to higher P-T conditions (methane-propane hydrate *vs.* pure propane hydrate, for example), and thus enabling more efficient reaction.

Regardless of which method is used, multiple cyclings through the melting point of ice are invariably required to ensure full reaction when using liquid hydrate-forming phases as reactants. Multiple P-T cyclings are particularly necessary for those systems in which the hydrate is stable to only several degrees above the melting point of ice. Our experience has shown that the length of time that such samples spend at warm temperature is less critical than for pure methane hydrate samples, and, instead, maximizing the number of cycles through the ice melting point drives the reaction more efficiently. Internal thermocouples are integral to such tests to establish the point at which melting and/or re-freezing anomalies cease to occur in the synthesis P-T record. Synthesis of methane-propane hydrate, for instance, requires approximately 5-7 cyclings over the duration of several days for complete reaction.

3. MEASUREMENT OF HYDRATE COMPOSITION AND STABILITY.

3.1 Gas flow meter and collection apparatus.

The volume, and hence mass of gas evolved from a dissociating sample, as well as the rate of gas evolution, can be measured with high precision in the gas flowmeter and collection apparatus shown in Figure 5 that is based on the principles of a Torricelli tube.

The apparatus consists of a closed-ended hollow cylinder made of stainless steel, inverted in a reservoir of distilled water, and suspended from a precision load cell. A column of water is initially drawn up by vacuum into the cylinder, and the weight of the cylinder plus water column is recorded as an initial baseline measurement. Maintenance of a constant drip rate into and out of the reservoir of water in which the cylinder is suspended ensures that the water level in the reservoir remains constant, and hence the buoyancy force on the cylinder remains constant. Methane is bubbled through the water to saturate it prior to dissociation, minimizing further methane solution during testing. Collection of a steady weight baseline is then made on the primed system, after which the hydrate sample can be opened to the flow meter.

As methane gas evolves from the dissociating sample and displaces water in the cylinder, the cylinder weight decreases. The mass of methane collected in the cylinder is then calculated from that weight change by incorporating additional run parameters into the data analysis, including: temperature inside the cylinder, atmospheric pressure, partial pressure of water vapor in methane, and the equation of state of methane gas. Calculation of the number of moles of methane can be simplified by using the ideal gas law, a procedure that accurately predicts the small relative changes of the sample pressure over the range of operation. The capacity of the flow meter shown in Figure 5 is 8 liters, and a typical methane hydrate sample made from 26 g of seed ice will release about 6 liters of gas during dissociation. Samples of the gas can then be collected for subsequent compositional analysis by attaching an evacuated receiving vessel to the vent/vacuum line. The flow meter operates with high accuracy at both high and low rates of gas flow, a result that we have verified over the range 0.01 to 3000 ml/min. Further details are provided by Circone et al., (2000).

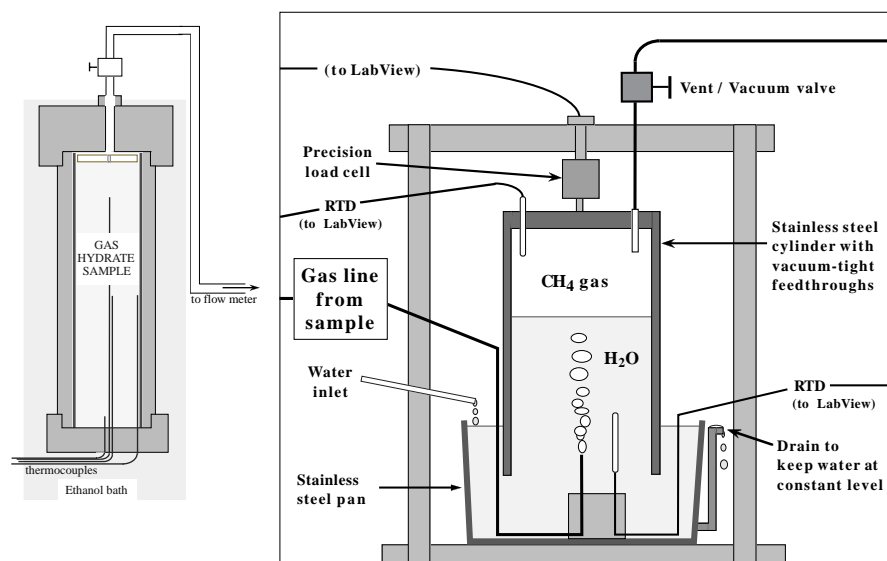


Figure 5. Gas flow meter and collection apparatus for measuring rates and amounts of gas released from dissociating samples. Flow rates may be measured over at least 5-orders of magnitude with excellent precision, while collecting the accumulating gas for mass measurement. Sample size relative to flow meter is not drawn to scale.

3.2 Dissociation procedures.

The most accurate measurement of the gas content evolving from dissociating hydrate are those made *in situ*, in which no quenching, depressurization, room-pressure handling, or sample re-installment onto the apparatus is required following synthesis. Either of two general procedures can be followed to take the hydrate samples from post-synthesis conditions of elevated methane pressure down to 0.1 MPa methane pressure prior to dissociation.

The first method, referred to as “temperature-ramping”, involves slow cooling of the external bath surrounding the samples while depressurizing the samples, remaining close to but just within the hydrate stability field (Fig. 6A, points 1-2-3). When the hydrate has cooled below 194 K, the remaining gas is vented to 0.1 MPa and the sample can be opened to the gas collection apparatus. Slowly warming the sample (by warming the external bath) above the methane hydrate dissociation temperature (194 K at 0.1 MPa) will then destabilize the hydrate, and the evolved gas is collected in the flow meter (Fig. 5). Warming the sample completely through the melting point of ice (273.15 K) then ensures full dissociation of the hydrate as well as full melting of the ice product that may trap residual amounts of hydrate or gas along grain boundaries or within grain interiors. Previously-quenched samples can also be dissociated by this method, by first cooling the external bath (to $T < 194$ K), and loading the quenched sample into a cold (< 194 K) vessel prior to reattachment to the apparatus.

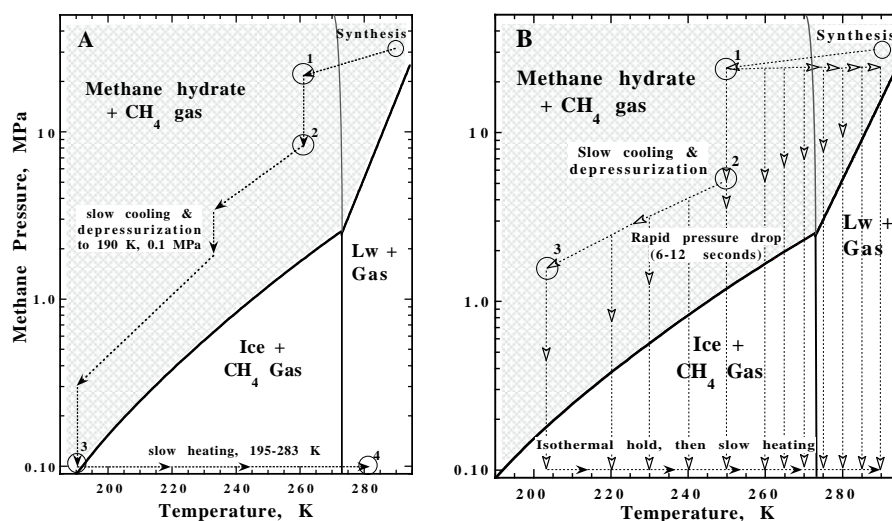


Figure 6. P-T paths for destabilizing methane hydrate for measurement of dissociation rates, stoichiometry, or stability behavior. Samples can be processed in two manners: (A) the “temperature ramping” method, or (B) the “rapid depressurization” method, each of which are effective for different types of dissociation tests. Procedures are described in the text.

The second dissociation method, termed “rapid depressurization”, involves first depressurizing the sample to a smaller overstep of the dissociation curve (Fig. 6B, pts. 1-2 or 3), then rapidly venting the pressure from several MPa above the equilibrium curve down to 0.1 MPa. The vent is then quickly closed while simultaneously opening the valve to the gas collection apparatus. The rapid depressurization is performed over about a 6 to 15 second interval, depending on the magnitude of the initial pressure overstep of the equilibrium curve. This technique is used to measure dissociation rates at a constant external bath temperature, and is particularly effective for isothermal warm-temperature tests to explore the P-T region where hydrate is predicted to dissociate to liquid

water + gas. For samples tested at temperatures above 195 K but below 273 K, it is necessary to warm the sample through 273 K after the isothermal portion of dissociation has finished, as in the temperature-ramping tests discussed above.

3.3 Stoichiometry measurements and annealing effects.

Stoichiometry measurements are ideally made on samples that are dissociated *in situ* directly after synthesis by the temperature-ramping procedures described above. This method permits stabilization of samples for an extended time at 0.1 MPa and at $T < 194$ K prior to dissociation, allowing the release of any residual pore gas or adsorbed methane on grain surfaces. Such release is easily detectable by baseline shifts recorded by the flow meter.

Seven samples tested in this manner confirmed the high reproducibility of sample composition produced by the prescribed growth methods; stoichiometry number n of all the test specimens measured at 5.89 ± 0.01 (Fig. 7A). This measured stoichiometry is slightly closer to ideal than that which we reported previously (6.1 ± 0.1 , on samples that contained 0 to 3 % unreacted ice, Stern et al., 1996) due to the greatly improved analytical and measurement capabilities provided by the internal thermocouples and the gas collection apparatus, and the current ability to detect very small amounts of unreacted ice. Samples are also now routinely held at the highest P-T conditions during synthesis for several hours longer than previously, to insure reaction of the last several percent of ice to hydrate. (The difference between n of 5.89 vs. 6.1 in methane hydrate samples corresponds to 3.2 vol. % unreacted ice.)

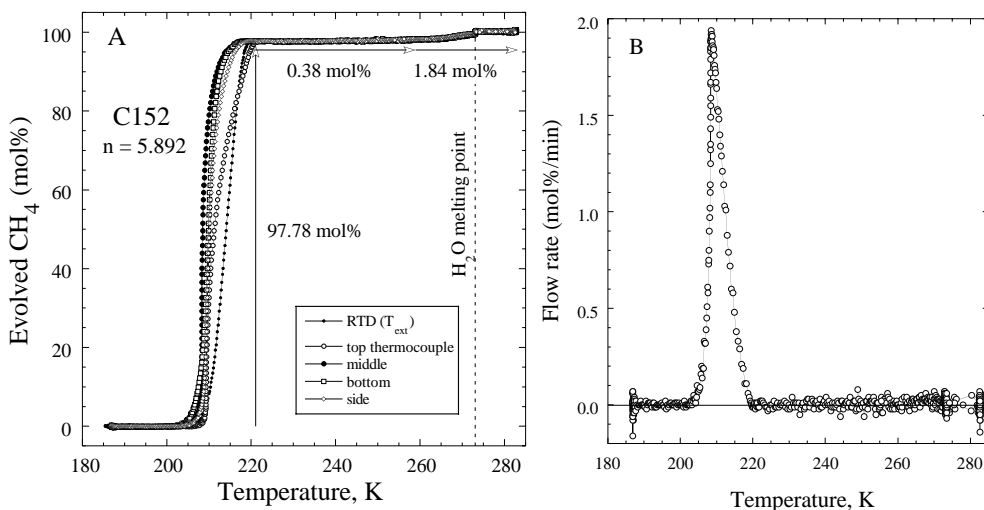


Figure 7. A typical dissociation profile (A) and flow-rate profile (B) for a sample of methane hydrate grown from 26 g of H_2O ice and dissociated by temperature-ramping procedures (Fig. 6A) by slowly warming the sample above dissociation conditions at a rate of approximately 11 K/hr. This sample yielded 0.244 moles of CH_4 gas, corresponding to a stoichiometry $\text{CH}_4 \cdot 5.89\text{H}_2\text{O}$. Most of the gas evolves over the temperature range 200 to 215 K, and the final 2-5% hydrate is not released until the sample is warmed through the H_2O melting point.

As our synthesis procedures form hydrate at conditions of P and T that are significantly overdriven with respect to the equilibrium curve, it may be desirable to anneal the as-grown hydrate at low P_{CH_4} or at equilibrium conditions prior to measurement of certain physical properties. Annealing is easily accomplished through resetting the P-T conditions on the samples to those more relevant to geologic settings, or to conditions close to or directly on the methane hydrate equilibrium curve (Fig. 1). Annealing effectively removes some methane from the hydrate structure (when made by the methods given here), as lower P stabilizes a less ideal stoichiometry. Kinetic factors are also important in reaching an equilibrium composition. On the laboratory time scale, there is a definite trade-off in achieving equilibrium compositions by reducing P at cold temperatures to very low equilibrium pressures, compared to annealing at warmer temperatures to the somewhat higher equilibrium pressures. While this effect has not yet been quantified, preliminary tests show that, as expected, annealing at warmer temperatures promotes a more rapid re-equilibration of n. Allowing a fully-reacted sample ($n = 5.89$) to anneal at 274 K and 4.5 MPa for 6 days, for instance, results in an increase in the stoichiometry number n to 6.01. Annealing at 250 K for 12 days at 2 MPa, however, only produces an increase in n to 5.94 even though the annealing pressure is lower (see Fig. 1).

3.4 Dissociation kinetics and phase stability.

The methods described above for *in situ* synthesis and stoichiometry measurement are particularly well suited for determination of effects of various pressure-temperature-time (P-T-t) paths on hydrate dissociation kinetics and phase stability, due to the ease of controlling such parameters as pressure, peak temperature, temperature-ramping rate, sample volume, sample composition, and stoichiometry. Below we present some representative results from nearly 100 experiments that demonstrate several applications of the flow meter to the investigation of hydrate dissociation kinetics and phase stability behavior over the temperature range 190 to 290 K at 0.1 MPa, as methane hydrate dissociates to either ice + CH_4 gas ($T < 273$ K) or liquid water + gas ($T > 273$ K).

3.4.1 Methane hydrate \rightarrow ice + gas. A suite of methane hydrate samples were removed from initially stable conditions of low T or elevated P by either the temperature-ramping method or the rapid-depressurization method discussed above. Samples decomposed by the temperature-ramping method exhibited highly reproducible decomposition behavior in which approximately 95% of the expected amount of gas evolved over the temperature range $195 \text{ K} < T < 220 \text{ K}$, as shown in Figure 7. The remaining gas was then only released from the samples (on the laboratory time scale) by warming through 273 K. This resistance to decomposition displayed by the residual 3-5% is likely due to its entrapment along ice grain boundaries or within grain interiors, as it is subsequently released by the melting of the encapsulating ice.

When rapidly depressurized at isothermal conditions ranging from 204 K to 240 K, methane hydrate samples exhibit systematically increasing dissociation rates with increasing temperature, as expected with the increasing

thermal overstep of the stability field (Fig. 8A). Samples tested at 204 K dissociated over ~ 3 hours, while those tested at 239 K dissociated within 7 minutes. These times correspond to the duration of the main dissociation event, or about 88-90 % reaction, and the remaining hydrate did not dissociate until the samples were warmed through 273 K and all the ice product had melted.

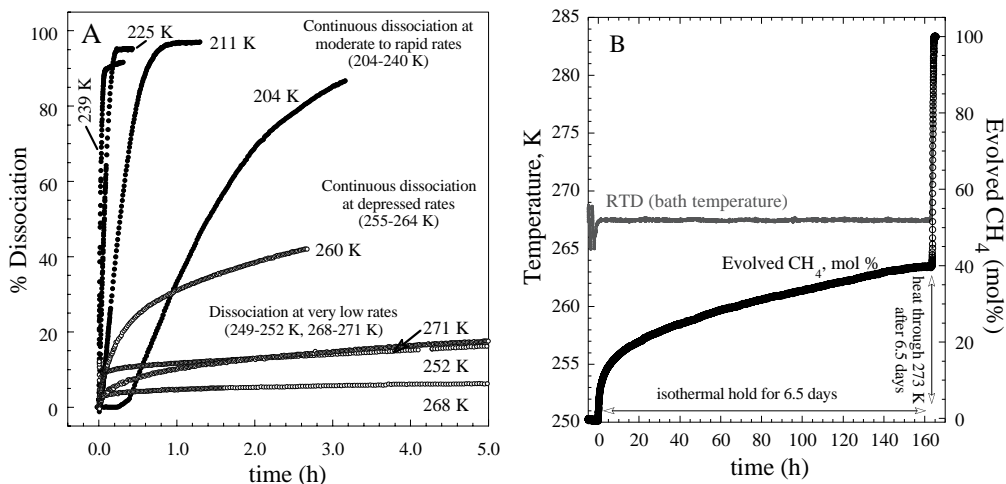


Figure 8. Representative curves from rapid depressurization tests, showing the unusual temperature dependency of methane hydrate dissociation kinetics as it decomposes to ice + gas. **(A)** Dissociation rates of samples tested over the temperature range 204 to 270 K. Up to 240 K, methane hydrate dissociates at increasing rates with increasing T. Only the isothermal portion of the tests are shown here; heating through 273 K then releases all remaining gas, usually totaling very close to 100% of the expected amount. From 250 to 270 K however, dissociation rates become highly suppressed, and large fractions of the hydrate can be "anomalously" preserved for at least many days. **(B)** Profile of a rapid depressurization test at 268 K, showing 60% of the hydrate preserving at 1 atm after 6 days, at temperatures 73 K above the equilibrium dissociation temperature. The expected remainder of gas was then recovered by heating the sample through 273 K.

"Anomalous" preservation" behavior. When methane hydrate samples are rapidly depressurized at isothermal conditions between 250 and 270 K, an anomalous preservation effect can be invoked (Fig. 8; also Stern et al., 1998c). This effect is most prominent at temperatures approaching 270 K, where significant amounts of hydrate can remain metastable due to greatly suppressed dissociation rates, even in tests lasting over 6 days (Fig. 8B). Warming of the metastable hydrate through 273 K then promotes full dissociation and rapid release of all remaining gas. Tests in which "preserved" samples were cooled to 190 K and then slowly rewarmed, however, showed that this preservation effect is thermally irreversible, as the samples then dissociated over the interval 198-218 K as observed in the temperature-ramping tests discussed above.

Based on textural observations of quenched samples and the lack of appreciable ice in them, it appears that warm-temperature preservation may be at least partially due to grain surface effects, grain boundary mobility, or structural

changes within the hydrate grains. This is in contrast to the residual hydrate in temperature-ramping tests that is released at 273 K, that is expected to be "preserved" by the encapsulating ice. Other tests conducted on unconsolidated methane hydrate and on hydrate + sediment \pm seawater mixtures, all samples that were rapidly depressurized at 268 K, demonstrated that while dissociation rates were less suppressed than those from more compacted or pure samples, the rates were still orders of magnitude slower than those predicted by extrapolation of dissociation rates from the lower temperature (204 to 240 K) regime. These results indicate that while the warm-temperature preservation effect is enhanced by grain boundary contacts, it is largely a structural or intrinsic property of methane hydrate.

We still do not fully understand the physical chemistry involved in this preservation effect, but have found it to be highly reproducible. Descriptions of other gas hydrate "self" preservation effects have also been documented by Davidson et al. (1986), Yakushev & Istomin, (1992), Gudmundsson et al. (1994), and Dallimore & Collett (1995).

3.4.2 Methane hydrate \rightarrow water + gas. Rapid-depressurization tests conducted at temperatures above 273 K show that dissociation proceeds in a systematic manner in which rates increase with increasing external temperatures (Fig. 9). In all tests conducted at $T > 273$ K, sample interior temperatures plummet and buffer at 272.5 K as dissociation proceeds (Fig. 9; also see Fig. 1 in Circone et al., 2000), an effect similar to that observed on recovered natural hydrate from oceanic drill core material (Kastner et al., 1995). Tests on methane hydrate + sediment \pm seawater samples also show that the addition of particulates and seawater both measurably increase the dissociation rate compared to pure hydrate samples. Additional details are provided by Circone et al., (2000).

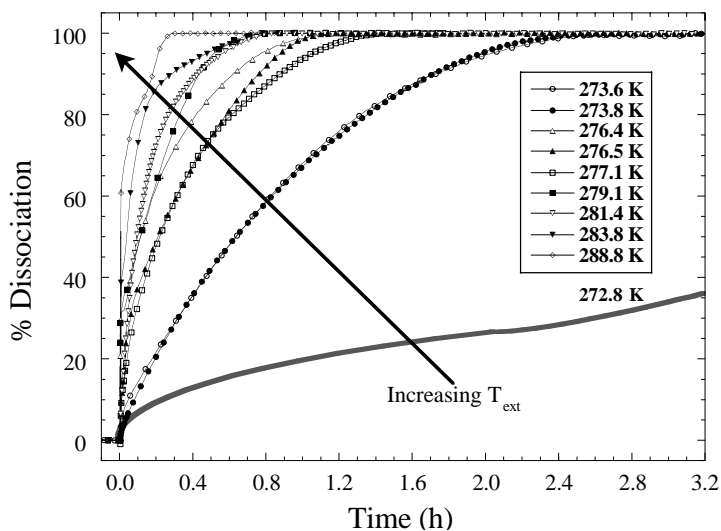


Figure 9. Dissociation rates of rapid depressurization tests conducted at $T > 273$ K, as pure methane hydrate decomposes to water + gas (from Circone et al., 2000, Fig. 2). With increasing external bath temperature (T_{ext}), dissociation rates increase systematically (shown by arrow). The two runs conducted at 273.6 K and 273.8 K demonstrate the excellent reproducibility of the test procedures and results.

4. APPLICATIONS FOR PHYSICAL PROPERTIES MEASUREMENT.

The methods described in this chapter for controlled growth of pure methane hydrate are particularly advantageous for further experiments that require either: (1) knowledge of sample purity, good control over P-T conditions and ease of modification of reaction vessel and apparatus specifications (for instance, annealing tests or measurement of gas-solid exchange, thermal conductivity, diffusivity, and acoustic property measurement), or (2) precise knowledge and control of grain characteristics (measurement of fracture strength and ductile flow behavior, for example). We review several modifications to our basic synthesis apparatus (Fig. 2) that we have used to acquire several of these types of measurements. Compaction procedures are also reviewed here, as many property measurements require precise knowledge of the sample porosity and the ability to remove all pore space from the test material.

4.1 Thermal conductivity.

The synthesis methods discussed in this chapter are well suited for experiments measuring thermal properties such as conductivity or diffusivity. Techniques developed by von Herzen and Maxwell (1959), for instance, can be adapted to measure thermal conductivity by use of a needle probe design that approximates an infinitely long, continuous line source of heat in an infinite medium. Cylindrical sample geometry can be modeled approximately as an infinite medium, and a needle probe placed along the axis of the sample can be approximated as a continuous line source of heat. Thermal conductivity of a sample can then be calculated directly by measuring the rise of temperature measured by the probe for a given heat input per unit length of wire per unit time, and for a given probe radius.

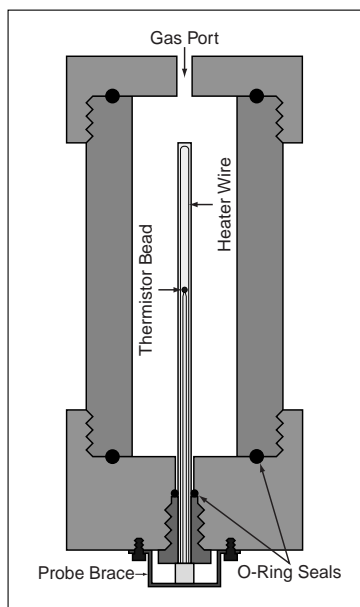


Figure 10. Schematic of sample chamber outfitted for hydrate growth followed by *in situ* thermal conductivity measurement using the needle probe technique. The probe is inserted through the base of the sample chamber prior to packing it with seed ice, and is supported from below by a metal brace to prevent probe expulsion from the chamber at elevated pressure. An O-ring seal around the probe prevents gas leakage through the insertion hole. The needle probe consists of an epoxy-filled hypodermic tube containing a 4 k Ω thermistor and a heater wire running the length of the probe. The probe has essentially the same length as the sample vessel, so departures from ideal cylindrical geometry during the heating phase of the experiment are negligible. Needle probe diameter is not drawn to scale.

The primary adjustment to the standard synthesis apparatus for such measurement involves replacing the standard sample vessel base with an endcap modified to accommodate the thermal probe, as shown in Figure 10. Preliminary success with this design has been reported by deMartin et al., (1999), in measuring thermal conductivity of pure methane hydrate samples and hydrate + quartz sand aggregates. Further discussion of the context of these measurements is provided by Ruppel et al., (this volume). Not only does *in situ* gas hydrate growth with the probe already in place ensure excellent contact between the hydrate and the probe, which is crucial to the success of this technique, but this method also avoids structural and stability problems inherent to drilling holes in quenched material for probe insertion. As this method measures thermal parameters of a porous aggregate, however, it is necessary to either establish the influence of the pore pressure medium on the measurements, or design a hydrostatic compaction capability around the sample to carefully compact and fully densify the material without damaging the probe. Such apparatus and procedural developments are currently in progress.

4.2 Compaction procedures.

Compaction of as-molded, porous material can be achieved by either uniaxial or hydrostatic compaction procedures. Our method for uniaxial compaction utilizes an apparatus that permits *in situ* synthesis, compaction, and elastic wave speed measurement (Fig. 11; see also Waite et al., 2000). This apparatus incorporates pistons at each end of the sample chamber, both of which are outfitted with a transducer assembly for wave speed measurement. The moving piston is advanced hydraulically to axially shorten the sample after synthesis, and the length change of the sample is monitored by the linear conductive plastic (LCP) transducer as shown in Figure 11.

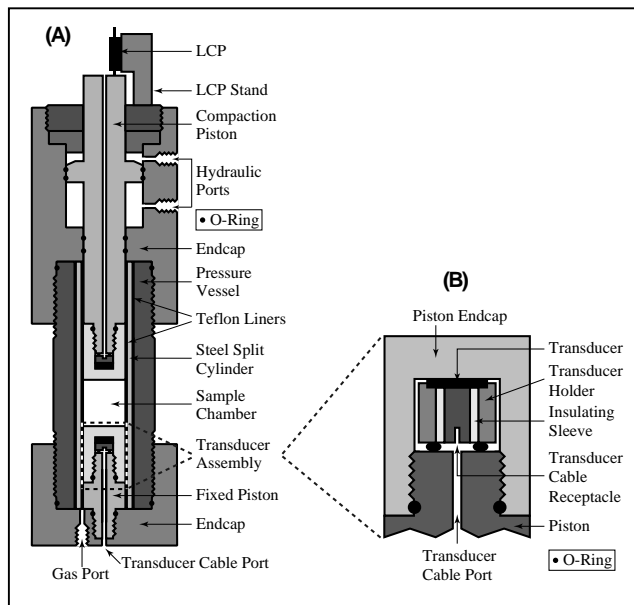


Figure 11. Gas hydrate synthesis apparatus equipped for subsequent *in situ* uniaxial compaction and measurement of acoustic wave speeds (from Waite et al., 2000).

(A) Pressure vessel schematic. Polycrystalline gas hydrate is synthesized directly in the sample chamber by the methods described in this chapter, then uniaxially compacted by hydraulically advancing the moving piston.

(B) Transducer assembly. Both pressure vessel pistons house a 1 MHz center-frequency piezoelectric transducer (either p- or s- wave), allowing pulse-transmission wave speed measurements to be made throughout the compaction process.

Prior to uniaxial compaction, the sample is vented to a pressure just sufficient to maintain it in its stability field; it is therefore beneficial to begin the compaction sequence at cold temperatures where hydrate is stable at lower pressures. Following this cold compaction, samples are partially repressurized and further compacted while raising the sample's temperature through the ice point. Compaction at high temperature facilitates elimination of the last percent of porosity, although the high strength of hydrate makes it increasingly difficult to achieve full compaction. Monitoring the wave speed profile throughout the compaction process provides independent determination of the presence or lack of any unreacted ice or water in the sample, as a measurable discontinuity in the wave speed can be measured if even trace amounts of H₂O freeze or melt.

For hydrostatic compaction (Fig. 12), a sample of gas hydrate is initially sealed in a soft jacket (such as indium metal) between two end caps or between an end cap and a force gauge, and pressurized from the outside with a confining medium gas. The sealing procedure must be performed at temperatures sufficiently cold to ensure stability of the hydrate. Hydrostatic compaction is best performed in an apparatus in which a piston can be advanced to touch and square the base of the sample, such as with the triaxial deformation apparatus shown in Figure 12. The confining pressure (P_c) is then slowly "stepped" up to 50 or 100 MPa in increments of roughly 20 MPa, taking care not to induce a high-pressure phase transformation in the samples at pressures just above 100 MPa (Chou et al., 2000). Following each compaction step, the piston is advanced to touch and square the bottom of the sample, then advanced just sufficiently to lightly compress the sample in order to compact it with minimal deformation. Optimally, the top end of the sample is attached to a gas line that can be either fully vented or maintained with a low CH₄ back pressure on the sample. Compaction can then be performed at either very cold conditions in the vented configuration, or at warmer temperatures with a regulated pore pressure.

4.3 Acoustic wave speed measurement.

Acoustic wave speed, the distance traveled by a wave divided by the wave's travel time, can be measured on hydrate grown directly in the uniaxial compaction apparatus shown in Fig. 11. Ultrasonic waves generated by the transducer in the compaction piston travel through the sample and are received by the transducer in the fixed piston. The travel time through the sample alone is given by the difference in the travel time between a signal passing through the complete system, and a "head-to-head" test signal sent from one transducer to the other when the pistons are in direct contact. The sample length is monitored using the LCP, and checked periodically by directly measuring the piston position relative to the pressure vessel.

In ice or gas hydrate samples, the signal to noise ratio is high enough to observe a distinct and measurable precursor compressional (p) wave generated by the shear (s) transducers. Using a pair of shear wave transducers, the compaction apparatus was successfully used to recover published wave speed values (V_p and V_s) for pure ice Ih, and also provided V_p and the first V_s results

for pure methane hydrate (V_p for methane hydrate was measured at 3650 ± 50 m/s, and V_s at 1890 ± 30 m/s; Waite et al., 2000). The simultaneous measurement of V_p and V_s also allows other additional elastic properties to be derived more reliably (see Helgerud et al., this volume).

4.4 Strength measurements.

Gas hydrate samples fabricated by the methods given in this chapter are also well suited for deformation testing in the type of apparatus shown in Figure 12. Because the composition and grain characteristics are well known and reproducible from sample to sample, such material is appropriate for rheological measurement and flow law characterization.

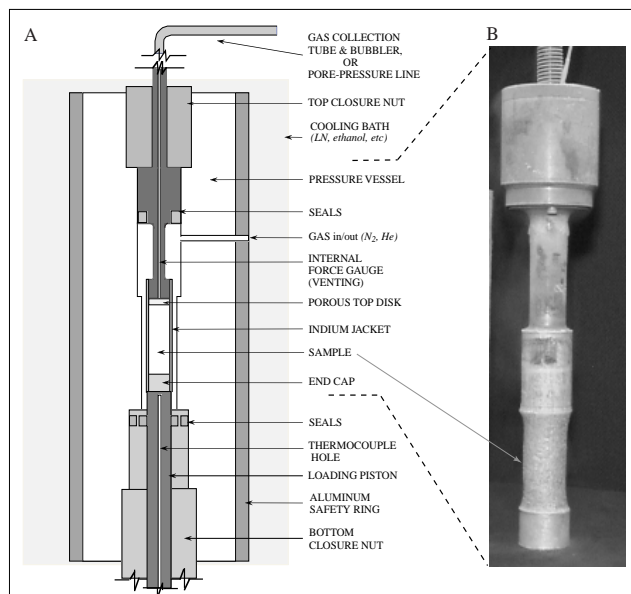


Figure 12. (A) Schematic of triaxial gas deformation apparatus used for hydrostatic compaction and subsequent deformation testing of gas hydrate test specimens. A jacketed sample (B) can be compacted and then measured for strength in compression tests, over the T range 77 to 300 K, at confining pressures up to 0.6 GPa, and strain rates 10^{-4} to 10^{-8} s $^{-1}$. The sample is attached to the internal force gauge, and a sliding piston moves through dynamic seals from below to impose axial shortening. A gas collection system or pore pressure line can be attached at the top of the apparatus to monitor possible methane loss during compaction and deformation, or to prevent gas hydrate decomposition.

The strength of methane hydrate samples has been measured in this laboratory in a suite of constant-strain-rates tests in compression, at conditions ranging from $T = 140$ to 287 K, confining pressure (P_c) of 50 to 100 MPa, and strain rates from 3.5×10^{-4} to 10^{-8} s $^{-1}$. The apparatus shown in Figure 12 is a 0.6-GPa gas deformation apparatus outfitted for cryogenic use (Heard et al., 1990) in which N_2 or He gas provides the P_c medium. The pressurized column within the apparatus consists of an internal force gauge, the jacketed sample, and a moving piston that compresses the sample axially against the internal force gauge at a fixed selected displacement rate. The soft indium jackets in which the samples were grown serve to encapsulate them during compaction and testing to exclude the P_c medium, and provide the additional benefit of superbly replicating the outer surface of the deformed sample, thus enabling subsequent microstructural study at room conditions (Fig. 10 in Stern et al. 1998a, for example). All gas hydrate samples tested in this apparatus were initially subjected to the hydrostatic pressurization and compaction sequence described above.

In tests conducted at $T < 200$ K, methane hydrate samples displayed strengths that were measurably but not substantially different from steady-state strengths of H_2O ice (Stern et al., 1996, 1998a). Recent tests conducted at warmer test conditions (>250 K), however, show that methane hydrate is enormously strong relative to water ice (Zhang et al., 1999, Durham et al., work in progress), a result which was not previously expected as water ice has commonly been assumed as a general proxy for the mechanical properties of gas hydrates. Figure 13 shows the relative strength differences between methane hydrate and pure water ice deformed in one of our first tests at 260 K, illustrating the dramatic strength differences. Further testing is currently underway to resolve better the strength and flow behavior of methane hydrate, and particularly to determine if possible shear instabilities or other solid-state processes are inherent to the deformation behavior (Stern et al., 1996, Durham et al., work in progress). Such instabilities not only increase the ice content of the sample with increasing strain, but mask the true strength of the pure hydrate due to the increasing ice contamination in the samples.

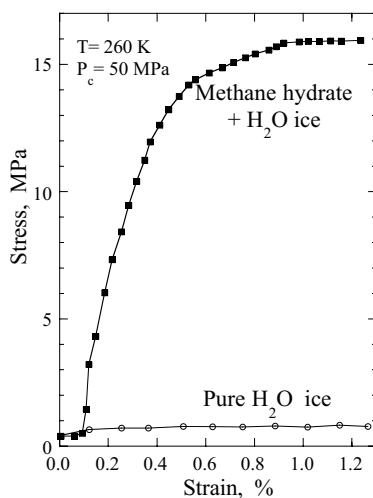


Figure 13. Comparison of the stress-strain histories of a mixed-phase sample of polycrystalline methane hydrate plus H_2O ice (approximately 3:1 volume ratio hydrate to ice), vs pure polycrystalline H_2O ice, at comparable test conditions. At lower temperature test conditions (< 200 K), the strength differences between methane hydrate and water ice are not significantly different, due to the high strength of both hydrate and ice at those conditions. At elevated temperatures as shown here, however, the strength contrasts are dramatic. Recent tests show that the strength of pure methane hydrate, even at $T > 273$, is at least several times stronger than that of the mixed-phase sample shown here (Durham et al., work in progress).

5. Summary and Conclusion.

Gas hydrates are challenging materials to investigate for physical properties. Water ice has proven to be a poor analogue material for methane hydrate, indicating that only measurements made directly on end-member gas hydrates will provide reliable results for use in quantitative models that evaluate the amounts of hydrate in sediments, or how gas hydrates may respond to gravitational loading, exchanges of heat, or changes in sea level. Synthesis or procurement of well-characterized and reproducible sample material is therefore crucial to the reliability and accuracy of such measurements.

We describe a simple method for making pure, cohesive, aggregates of methane hydrate that may be easily reproduced in any laboratory. Compositional measurements using a unique precision gas flow meter indicate that the

stoichiometry of the resulting material is closely reproducible at $\text{CH}_4 \bullet n\text{H}_2\text{O}$ where $n = 5.89 + 0.01$. Grain size, porosity and aggregate cohesion are also closely reproducible, and the specimen shape is primarily limited by the shape into which granular ice may be packed. Customized aggregates of hydrate-sediment mixtures, or hydrates with mixed hydrocarbon phases, can also be easily manufactured by our *in situ* "seeding" method. Our experience has also shown that by combining methods of synthesis, compaction, and property measurement in a single reaction vessel, it is possible to avoid the structural, compositional, and reproducibility problems that plague experiments that rely on 1-atm sample handling and cold transfer procedures.

Several key findings and results have emerged from this line of research. Direct and precise measurement of the shear and compressional wave speeds have now been made *in situ* on compacted samples on pure, polycrystalline methane hydrate, for example. These end-member values should prove useful in making more quantitative inferences of gas hydrate content in sediment columns as determined from conventional sonic well logs, vertical seismic profiling, or those inferred from arrivals from explosion or surface airgun sources.

Decomposition rates of pure, porous methane hydrate have also been systematically measured at 1 atm over the temperature range 195 K to 290 K, resulting in the unexpected discovery of a warm-temperature thermal regime (250-270 K) where methane hydrate can remain metastably preserved for extended periods of time. This preservation effect may have important applications to strategies used for retrieval of natural hydrates from drill core, as well as for gas yield rates in hydrate exploitation schemes using pressure release methods to decompose the hydrate.

Another unexpected finding is that pure methane hydrate has a markedly higher plastic flow strength than ice at terrestrially-relevant conditions. The high strength of methane hydrate extends to well above 273 K where water is in liquid form. If gas hydrate serves as a cementing agent in hydrate-bearing sediments, such aggregates should be stronger than permafrost. Hydrate decomposition due to depressurization or heating, as caused by a decrease in sea level or by hot oil extraction from below the gas hydrate interval, could therefore cause large changes in the slope stability of sediments on continental margins, or in the near-surface strength of sediments under drilling platforms.

Lastly, the successful adaptation of the needle-probe method for direct *in situ* measurement of the thermal conductivity of pure, porous methane hydrate confirms that conductivity is extremely low relative to ice and to granular (detrital) sediments. Further measurement on fully dense methane hydrate will provide the additional information on heat transfer properties that is essential for quantitative modeling of the effects of gas hydrate on climate change, and for evaluating the effects of coring and deep oil extraction through gas-hydrate-bearing sediments.

References

- Chou, I. M., Burress, R., Goncharov, A., Sharma, A., Hemley, R., Stern, L., & Kirby, S. 2000. *In situ* observations of a new high-pressure methane hydrate phase. *Eos, Trans. Amer. Geophys. Union*, in press.
- Chou, I. M., Pasteris, J., & Seitz, J. 1990. High density volatiles in the system C-O-H-N for the calibration of a laser Raman microprobe. *Geochimica Cosmochimica Acta*, 54, 535-543.
- Circone, S., Stern, L.A., Kirby, S. H., Pinkston, J. C., & Durham, W. B. 2000. Pure methane hydrate dissociation rates at 0.1 MPa and temperatures above 272 K, *Annals of the New York Academy of Sciences*, 3rd International Conference on Gas Hydrates, in press, 20 pp.
- Dallimore, S. R., & Collett, T. S. 1995. Intrapermafrost gas hydrates from a deep core hole in the Mackenzie Delta, Northwest Territories, Canada. *Geology*, 23, 6, 527-530.
- Davidson, D. W., Garg, S. K., Gough, S. R., Handa, Y. P., Ratcliffe, C. I., Ripmeester, J. A., & Tse, H. S. 1986. Laboratory analysis of a naturally occurring gas hydrate from sediment of the Gulf of Mexico. *Geochim. Cosmochim. Acta*, 50, 619-623.
- DeMartin, B., Waite, W., Ruppel, C., Pinkston, J., Stern, L., & Kirby, S. 1999. Laboratory thermal conductivity measurements of methane hydrate and hydrate-sediment mixtures under simulated *in situ* conditions. *Eos, Trans. Am.er. Geophys. Union*, 80, 17, S337.
- Durham, W. B., Heard, H. C., & Kirby, S. H. 1983. Experimental deformation of polycrystalline H₂O ice at high pressure and low temperature: preliminary results, *J. Geophys. Res.*, 88, B377-B392.
- Durham, W.B. Kirby, S.H., & Stern, L.A. 1993. Flow of ices in the ammonia-water system, *Journal of Geophysical Research*, 98 (B10), 17,667-17,682.
- Gudmundsson, J. S., Parlaktuna, M., & Khokhar, A. A. 1994. Storing natural gas as frozen hydrate. *SPE Production and Facilities*. 69-73.
- Heard, H., C., Durham, W. B., Boro, C., & Kirby, S. H. 1990. A triaxial deformation apparatus for service at $77 \leq T \leq 273$ K, in: *The Brittle-Ductile Transition in Rocks*, Geophysical Monograph 56, ed. by A. G. Duba et al., American Geophysical Union, Washington, D. C., 225-228.
- Kastner, M., Kvenvolden, K. A., Whiticar, M. J., Camerlenghi, A., & Lorenson, T. D. 1995. Relation between pore fluid chemistry and gas hydrates associated with bottom-simulating reflectors at the Cascadia Margin, sites 889 and 892. *Proc. of the Ocean Drilling Program, Scientific Results*, 146, 1, 175-187.

- Moudrakovski, I. L., Ratcliffe, C. I., McLaurin, G. E., Simard, B., & Ripmeester, J. A. 1999. Hydrate layers on ice particles and superheated ice: a ^1H NMR microimaging study". *J. Phys. Chem. A*, 103, 4969-4971.
- Sloan, E., D Jr. *Clathrate Hydrates of Natural Gases*, 2nd Edition, Marcel Dekker, Inc., New York, 1998, 705 pp.
- Stern, L. A., Kirby, S. H., & Durham, W. B. 1996, Peculiarities of methane clathrate hydrate formation and solid-state deformation, including possible superheating of water ice, *Science*, 273, 5283, 1843-1848.
- Stern, L. A., Kirby, S.H., & Durham, W. B. 1998a. Polycrystalline methane hydrate: synthesis from superheated ice, and low-temperature mechanical properties, *Energy & Fuels*, 12, 2, 201-211.
- Stern, L. A., Hogenboom, D. L., Durham W. B., Kirby S. H., & Chou I-M. 1998b. Optical cell evidence for superheated ice under gas-hydrate-forming conditions, *J. Phys. Chem. B*, 102, 15, 2627-2632.
- Stern, L. A., Circone, S., Kirby, S. H., Pinkston, J. C., & Durham, W. B. 1998c, Dissociation of methane hydrate at 0.1 MPa, and short term preservation by rapid depressurization. *EOS*, Transactions of the American Geophysical Union, 79, 45, 462.
- Von Herzen, R. & Maxwell, A. E. 1959. The measurement of thermal conductivity of deep-sea sediments using the needle-probe method, *J. Geophys. Res*, 64, 1557-1563.
- Waite, W. F., Helgerud, M. B., Nur, A., Pinkston, J.C., Stern, L. A., Kirby, S. H., & Durham, W. B. 2000. Laboratory measurements of compressional and shear wave speeds through pure methane hydrate, *Annals of the New York Academy of Sciences*, 3rd International Conference on Gas Hydrates, in press, 8 pp.
- Zhang, W, Durham, W.B., Stern, L. A., & Kirby, S. H. 1999. Experimental deformation of methane hydrates: new results. *Eos*, Trans. Amer. Geophys. Union, 80, 17, S337.